Electron Density Analysis of Substituted Carbonyl Groups†

David L. Grier and Andrew Streitwieser, Jr.*

Contribution from the Department of Chemistry, University of California, Berkeley, California 94720. *Received July 13, 1981*

Abstract: Ab initio LCAO-SCF-MO methods have been used to produce projected electron density difference maps for a series of substituted carbonyls, with formaldehyde as reference. Numerical integration of the region about oxygen yields difference integrated spatial electron populations (ΔISEP) for both π- and σ-electronic systems. These electronic changes are used to investigate the behavior of various substituents on the carbonyl group for comparison with conventional concepts in the electronic theory of organic chemistry. The results show generally the effects of primary polarization in the π system and a back-polarization induced in the σ system. The net changes at oxygen are much smaller; that is, changes given by integrating a sphere around oxygen would be small and do not reveal the underlying polarization mechanisms. the ΔISEPs found are also compared with Mulliken populations, with Hammett-type σ parameters, and with oxygen 1s orbital energies.

The concept of "atomic charge" has been of central importance in the development of chemistry; yet it has no rigorous definition and must be empirically determined. In terms of quantum mechanical investigations, the simplest scheme for assigning charge has been to partition the electron density according to contributions from the mathematical functions comprising the basis set; this is the foundation for the well-known Mulliken population analysis[1] and its variants,[2] which differ primarily in the mode of partitioning of the overlap density. The important weakness with this type of analysis is that the electron density associated with a given basis function is assigned to the atom on which that function is centered, even if that function has significant amplitude near some other atomic center.

Direct integration of the electron density function alleviates this weakness but poses a further question: how does one define the region over which to integrate? For linear (or quasi-linear) systems the covalent radius (or $^1/_2$ the homonuclear distance) of a given atom is one obvious choice;[3] recently, Wiberg[4] has expanded this approach to include a tetrahedral region about carbon in more complex nonlinear molecules. Another obvious choice for linear systems is to define each atom on the basis of the minimum[3b,5] in the electron density function between the atoms; this has also been expanded to three dimensions by Bader.[6,7n] The boundaries so defined mark atomic regions as "virial fragments" that have unique and significant properties. Other definitions have been proposed;[7] for example, one can define regions on the basis of a superposition of free atom electron densities.[7a-f]

In applying the concepts of physical organic chemistry, we are generally concerned not with absolute quantities but with the *change* induced by a *change* in structure. A common example is the use of curved arrows to represent intramolecular charge transfer. In the present context of the effect of structure on the electronic character of the carbonyl group, we would be concerned with the difference electron density function for a carbonyl compound relative to a standard such as formaldehyde. Such a difference function generally shows significant changes at oxygen and carbon but only small and gradual changes in the internuclear region; hence, integrated *difference* populations are expected to be less sensitive to the precise boundary definition used. This philosophy of using difference functions is adopted in this paper and is implemented by the use of the electron density projection function, $P(x,z)$:[5a,8]

$$P(x,z) = \int_{-\infty}^{+\infty} \rho(x,y,z)\, dy \qquad (1)$$

This function is used to examine changes in integrated electron density about the carbonyl oxygen, as we subtract the electron density projection function of formaldehyde from that of various substituted aldehydes and ketones. The result is a difference integrated spatial electron population, ΔISEP.

Methods

The procedure we follow is to first compute[8] a projection function density difference contour map; for example, Figure 1 displays the projection function difference $P(CH_3CHO) - P(H-$

† This paper is dedicated to the 65th birthday (June 22, 1982) of Professor William von E. Doering, who gave the senior author his first instruction in the electronic theory of organic chemistry.

(1) (a) Mulliken, R. S. *J. Chem. Phys.* **1955**, *23*, 1833-1840, 1841-1846, 2338-2342, 2343. (b) Mulliken, R. S. *Ibid.* **1961**, *36*, 3428-3439. (c) Mulliken, R. S. *Ibid.* **1951**, *19*, 1614-1615.

(2) (a) Peters, D. *J. Chem. Soc.* **1963**, 2015-2023. (b) Cusachs, L. C.; Politzer, P. *Chem. Phys. Lett.* **1968**, *1*, 529-531. (c) Cusachs, L. C.; Politzer, P. *Ibid.* **1968**, *2*, 1-4. (d) Davidson, E. R. *J. Chem. Phys.* **1967**, *46*, 3320-3324. (e) Lowdin, P. O. *Ibid.* **1950**, *18*, 365-375. (f) Doggett, G. *J. Chem. Soc. A* **1969**, 229-233. (g) Lowdin, P. O. *J. Chem. Phys.* **1953**, *21*, 374-375. (h) Pollak, M.; Rein, R. *Ibid.* **1967**, *47*, 2045-2052. (i) Politzer, P.; Mulliken, R. S. *Ibid.* **1971**, *55*, 5135-5136. (j) Stout, E. W., Jr.; Politzer, P. *Theor. Chim. Acta* **1968**, *12*, 379-386. (k) Hillier, I. H.; Wyatt, J. F. *Int. J. Quantum Chem.* **1969**, *3*, 67-71. (l) Yanez, M.; Stewart, R. F.; Pople, J. A. *Acta Crystallogr., Sect. A* **1978**, *A34*, 641-648. (m) Roby, K. R. *Mol. Phys.* **1974**, *27*, 81-104. (n) Paoloni, L. *J. Chem. Phys.* **1959**, *30*, 1045-1058. (o) Coulson, C. A.; Doggett, G. *Int. J. Quantum Chem.* **1968**, *2*, 825-843. (p) Ros, P.; Schuit, G. C. A. *Theor. Chim. Acta* **1966**, *4*, 1-12. (q) Christoffersen, R. E.; Baker, K. A. *Chem. Phys. Lett.* **1971**, *8*, 4-9.

(3) (a) Bader, R. F. W.; Henneker, W. H.; Cade, P. E. *J. Chem. Phys.* **1967**, *46*, 3341-3363. (b) Lischka, H. *J. Am. Chem. Soc.* **1977**, *99*, 353-360. (c) Dean, S. M.; Richards, W. G. *Nature (London)* **1975**, *256*, 473-475.

(4) Wiberg, K. B. *J. Am. Chem. Soc.* **1980**, *102*, 1229-1237.

(5) (a) Streitwieser, A. Jr.; Williams, J. E.; Alexandratos, S.; McKelvey, J. M. *J. Am. Chem. Soc.* **1976**, *98*, 4778-4784. (b) Boyd, R. J. *J. Chem. Phys.* **1977**, *66*, 356-358. (c) Politzer, P.; Reuther, J.; Kasten, G. T. *Ibid.* **1977**, *67*, 2385-2387. (d) Bader, R. F. W.; Beddall, P. M. *Chem. Phys. Lett.* **1971**, *8*, 29-36.

(6) (a) Bader, R. F. W.; Beddall, P. M.; Cade, P. E. *J. Am. Chem. Soc.* **1971**, *93*, 3095-3107. (b) Bader, R. F. W.; Beddall, P. M. *Ibid.* **1973**, *95*, 305-315. (c) Bader, R. F. W. *Acc. Chem. Res.* **1975**, *8*, 34-40. (d) Bader, R. F. W.; Anderson, S. G.; Duke, A. J. *J. Am. Chem. Soc.* **1979**, *101*, 1389-1395. (e) Bader, R. F. W.; Beddall, P. W. *J. Chem. Phys.* **1972**, *56*, 3320-3329. (f) Bader, R. F. W.; Beddall, P. M.; Peslak, J., *Jr. Ibid.* **1973**, *58*, 557-566. (g) Bader, R. F. W.; Messer, R. R. *Can. J. Chem.* **1974**, *52*, 2268-2282.

(7) (a) Politzer, P.; Harris, R. R. *J. Am. Chem. Soc.* **1970**, *92*, 6451-6460. (b) Politzer, P. *Theor. Chim. Acta* **1971**, *23*, 203-207. (c) Politzer, P.; Reggio, P. H. *J. Am. Chem. Soc.* **1972**, *94*, 8308-8311. (d) Ransil, B. J.; Sinai, J. J. *Ibid.* **1972**, *94*, 7268-7276. (e) Politzer, P.; Elliott, J. D.; Meroney, B. F. *Chem. Phys. Lett.* **1973**, *23*, 331-334. (f) Politzer, P.; Politzer, A. *J. Am. Chem. Soc.* **1973**, *95*, 5450-5455. (g) Bader, R. F. W.; Bandrauk, A. D. *J. Chem. Phys.* **1968**, *49*, 1653-1665. (h) Politzer, P.; Harris, R. R. *Tetrahedron* **1971**, *27*, 1567-1572. (i) Bader, R. F. W.; Keaveny, I.; Cade, P. E. *J. Chem. Phys.* **1967**, *47*, 3381-3402. (j) Ransil, B. J.; Sinai, J. J. *Ibid.* **1967**, *46*, 4050-4074. (k) Brown, R. E.; Shull, H. *Int. J. Quantum Chem.* **1968**, *2*, 663-685. (l) Daudel, R.; Brion, H.; Odiot, S. *J. Chem. Phys.* **1955**, *23*, 2080-2083. (m) Russeger, P.; Schuster, P. *Chem. Phys. Lett.* **1973**, *19*, 254-259. (n) Daudel, R.; Bader, R. F. W.; Stephens, M. E.; Barrett, D. S. *Can. J. Chem.* **1974**, *52*, 1310-1320. (o) Doggett, G. *Mol. Phys.* **1977**, *34*, 1739-1757. (p) Polak, R. *Theor. Chim. Acta* **1978**, *50*, 21-30. (q) Iwata, S. *Chem. Phys. Lett.* **1980**, *69*, 305-312.

(8) (a) Streitwieser, A., Jr.; Collins, J. B.; McKelvey, J. M.; Grier, D.; Sender, J.; Toczko, A. G. *Proc. Natl. Acad. Sci. U.S.A.* **1979**, *76*, 2499-2502. (b) Collins, J. B.; Streitwieser, A. Jr.; *J. Comput. Chem.* **1980**, *1*, 81-87. (c) Collins, J. B.; Streitwieser, A.; Jr.; MeKelvey, J. M. *Comput. Chem.* **1979**, *3*, 79.

0002-7863/82/1504-3556$01.25/0

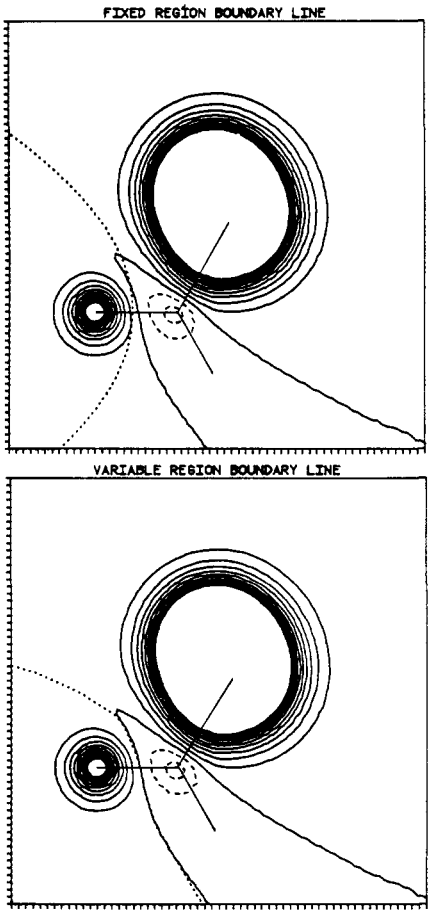

Figure 1. $P(CH_3CHO) - P(HCHO)$ for π electrons. Contours are from −0.005 to 0.025 by 0.0025 e/au^2. Dotted line is integration boundary about oxygen. In all contour maps, oxygen is at the left while the substituent (in this case methyl) is in the upper right. Negative contours are dashed; the zero contour is the first solid contour.

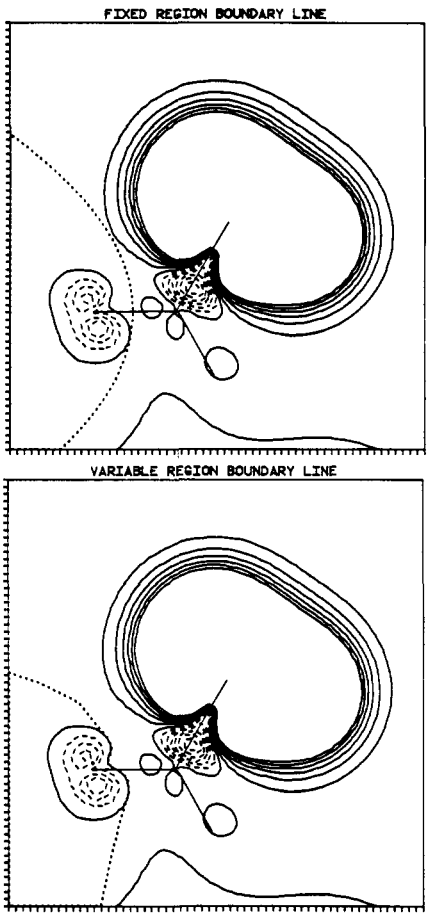

Figure 2. $P(CH_3CHO) - P(HCHO)$ for σ electrons. Contours are from −0.018 to 0.018 by 0.003 e/au^2.

CHO) for π electrons. Next, from such a contour map we define a region about the oxygen atom within which we can determine the number of electrons by a simple numerical integration of the contour map grid data. It should be noted that this procedure yields a "difference integrated spatial electron population", ΔISEP, and corresponds to the integration

$$\Delta\text{ISEP} = \int\int_{\substack{x,z \\ \epsilon S}}\int_{-\infty}^{+\infty} \rho(x,y,z)\, dy\, dx\, dz \qquad (2)$$

where S is a closed surface that is a function of x and z only and is the region that is used to define the oxygen.

In this study we have chosen two such regions. Figures 1–3 denote these regions as dotted lines on some typical difference maps: acetaldehyde minus formaldehyde (π, σ, and valence systems). The first (hereafter called "variable") region depends upon the density difference map being studied and is defined on the right by the zero contour line passing between carbon and oxygen and on the left by the edges of the contour map. Since these edges are rather far from the oxygen, there is rather little "leakage" off the edge of the plot; the figures typically include 99.8% of the total electrons. This definition approximates a difference density analogue of Bader's "virial fragment"; since our region extends to $\pm\infty$ in the y direction, the analogy is not complete. Indeed, our definition is intermediate between the virial boundary of Bader and Beddall[6e] and the "natural partitioning" of Bader, Beddall, and Cade.[6a] The latter is a perpendicular plane between atoms in a diatomic molecule compared to our current vertical partitioning "curtain". In the present context the differences among the various definitions involve regions of small electron density differences and should give quantitatively similar results. We further note that the use of a variable boundary separately for π, σ, and valence regions implies that the sum $P(\pi$ difference) plus $P(\sigma$ difference) does not, in general, equal P-(valence difference), although it is often very close. Note that the contours do show rather shallow changes at these boundaries.

The second region we have examined (hereafter called "fixed") is constant for all of the molecules treated and is defined on the right by a parabola that passes through the covalent radius of the CO double bond (0.55 Å from oxygen).[9] Again, the left-hand boundary is defined by the edge of the contour map. This fixed region corresponds reasonably well with the variable region; along the CO double bond the average difference between the two is 0.04 Å.

The use of variable boundaries provides a valuable additional comparison; thus, we have chosen to use these numbers in our discussion. It is important to note, however, that none of the conclusions is affected significantly by this choice. This result was to be expected by our fundamental philosophy of using *difference* functions; the contours show rather shallow changes at the boundaries, and conclusions are not sensitive to the precise definition of boundary used so long as the boundary is in this general region.

Since the "core" MOs are contained essentially wholly within the defined boundaries, integrations were confined to occupied "valence" MOs, that is, with MOs corresponding to the core orbitals of heavy elements excluded. All of the molecules examined have a plane of symmetry that includes the HCO or CO group; accordingly all MOs are either symmetric (σ) or antisymmetric (π) with respect to this plane.

The substituents of the substituted aldehydes studied were CH_3, BH_2, $CH{=}CH_2$, CCH, CHO, NH_3^+, BH_3^-, CH_2^-, F, OH, SH, CN, $NH_{2\parallel}$ (planar with lone pair parallel to the π system), and $NH_{2\perp}$ (planar with lone pair perpendicular to the π system). We

(9) Hine, J. "Physical Organic Chemistry"; McGraw-Hill: New York, 1956; p 30.

Table I. 4-31G Difference Populations on Oxygen: ΔISEP (*P*(Substituted Aldehyde (Ketone)) − *P*(Formaldehyde)) (electrons)

substituent	variable region π	variable region σ	variable region valence	fixed region π	fixed region σ	fixed region valence
			Aldehydes			
H	0.000	0.000	0.000	0.000	0.000	0.000
F	0.076	−0.079	−0.003	0.075	−0.077	−0.002
$NH_2\parallel$	0.198	−0.071	0.126	0.198	−0.069	0.128
$NH_2\perp$	0.018	−0.020	0.009	0.017	−0.041	0.003
NH_3^+	−0.047	−0.067	−0.112	−0.047	−0.065	−0.112
CH_3	0.047	−0.016	0.040	0.047	−0.009	0.037
BH_3^-	0.119	0.011	0.141	0.119	0.019	0.138
BH_2	−0.060	0.036	−0.024	−0.059	0.038	−0.021
OH	0.142	−0.077	0.069	0.141	−0.068	0.074
SH	0.076	−0.054	0.024	0.075	−0.049	0.027
CN	−0.023	−0.020	−0.043	−0.022	−0.021	−0.043
CHO	−0.020	0.002	−0.019	−0.019	0.003	−0.016
CH_2^-	0.321	−0.062	0.284	0.321	−0.048	0.273
$CHCH_2$	0.051	−0.013	0.041	0.052	−0.011	0.041
CCH	0.019	−0.016	0.003	0.019	−0.019	0.000
			Ketones			
ketene	0.161	−0.202	−0.040	0.161	−0.201	−0.040
cyclopropanone	0.066	−0.063	0.001	0.065	−0.061	0.004
cyclopropenone	0.230	−0.156	0.080	0.230	−0.150	0.080
acetone	0.087	−0.026	0.073	0.086	−0.015	0.072

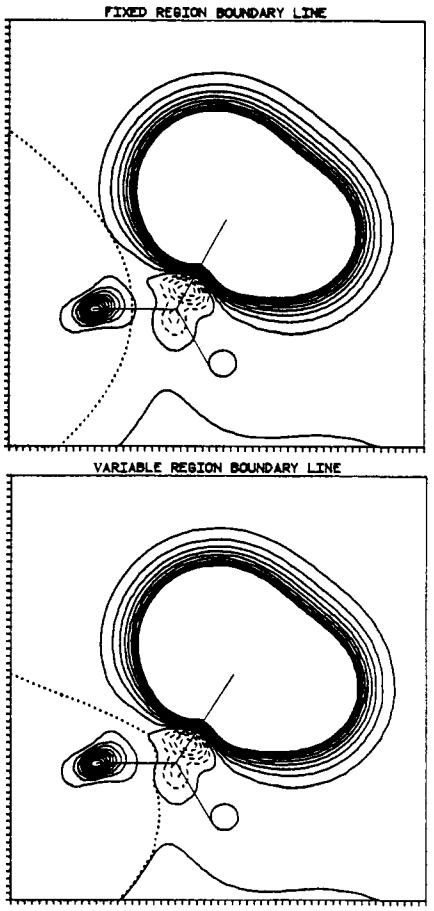

Figure 3. $P(CH_3CHO) - P(HCHO)$ for valence electrons. Contours are from −0.012 to 0.027 by 0.003 e/au^2.

also looked at the ketones acetone, ketene, cyclopropanone, and cyclopropenone. All ab initio calculations were performed by using the 4-31G basis set, with either GAUSSIAN-70,[10] GAUSSIAN-76,[10] or HONDO.[10] Standard geometries were used, with certain exceptions.[11] Note that in order to derive difference electron densities it is essential that the same C=O bond distance be used throughout; otherwise, changes close to the nuclei will seriously complicate the interpretation. We recognize that this bond length

Table II. 4-31G Mulliken Difference Populations on Oxygen: (*P*(Substituted Aldehyde (Ketone)) − *P*(Formaldehyde))

substituents	population π	population σ	population valence
	Aldehydes		
H	0.000	0.000	0.000
F	0.081	−0.077	0.005
$NH_2\parallel$	0.202	−0.069	0.134
$NH_2\perp$	0.014	−0.023	−0.009
NH_3^+	−0.061	−0.070	−0.131
CH_3	0.044	−0.007	0.037
BH_3^-	0.130	0.032	0.161
BH_2	−0.067	0.060	−0.006
OH	0.150	−0.077	0.074
SH	0.076	−0.071	0.005
CN	−0.030	−0.014	−0.044
CHO	−0.024	0.018	−0.006
CH_2^-	0.334	−0.034	0.300
$CHCH_2$	0.051	0.009	0.060
CCH	0.015	−0.018	−0.003
	Ketones		
ketene	0.169	−0.091	0.078
cyclopropanone	0.058	−0.012	0.046
cyclopropenone	0.233	−0.098	0.135
acetone	0.080	−0.007	0.073

(10) (a) Hehre, M. J.; Lathan, W. A.; Ditchfield, R.; Newton, M. D.; Pople, J. A. *QCPE* **1973**, 236. (b) Binkley, J. S.; Whitehead, R. A.; Hariharan, P. C.; Seeger, R.; Pople, J. A.; Hehre, W. J.; Newton, M. D. *Ibid.* **1978**, 368. (c) Dupuis, M.; Rys, J.; King, H. F. *Ibid.* **1977**, 336.

(11) (a) Pople, J. A.; Gordon, M. *J. Am. Chem. Soc.* **1967**, *89*, 4253–4261. (b) Dill, J. D.; Schleyer, P. von R.; Pople, J. A. *Ibid.* **1975**, *97*, 3402–3409. Exceptions are as follows: NH_3^+, N–H = 1.03 Å (from NH_4^+),[12b] C–N = 1.48 Å (from $CH_3NH_3^+$);[12b] BH_3^-, B–H = 1.25 Å (from BH_4^-),[12a] C–B = 1.64 Å (from various Ph_4B^- salts and $LiB(CH_3)_4$);[13] CH_2^-, the C–C bond was lengthened to that of acetaldehyde, so that a comparison between these two molecules could be made; cyclopropenone, C=O = 1.22 Å (standard) (the rest of the molecule is from the microwave structure);[14] cyclopropanone, C=O = 1.22 Å (standard) (the rest of the molecule is from the crystal structure).[15]

(12) (a) "Tables of Interatomic Distances and Configuration in Molecules and Ions"; The Chemical Society: London, 1958, Special Publication No. 11. (b) "Tables of Interatomic Distances and Configuration in Molecules and Ions: Supplement 1956–1959"; The Chemical Society: London, 1965, Special Publication No. 18.

(13) (a) Rhine, W. E.; Stucky, G.; Peterson, S. W. *J. Am. Chem. Soc.* **1975**, *97*, 6401–6406. (b) Domenico, A.; Vaciago, A. *Acta Crystallogr., Sect. B* **1975**, *B31*, 2553–2554.

(14) Benson, R. C.; Flygare, W. H.; Oda, M.; Breslow, R. *J. Am. Chem. Soc.* **1973**, *95*, 2772–2777.

(15) Pochan, J. M.; Baldwin, J. E.; Flygare, W. H. *J. Am. Chem. Soc.* **1969**, *91*, 1896–1898.

does change somewhat from compound to compound, but such small variations are not expected to have any significant effect on the qualitative interpretations.

Projection function calculations were performed with PROJ;[8c] the grid line spacing was 0.2 au in both x and z directions.[16] The numerical integrations for the oxygen regions were performed with a BASIC program on a Tektronix 4051 microcomputer.

Results

A complete set of the contour maps for all of the compounds studied is available as supplementary material.[17] As noted above, Figures 1–3 display several of these maps, which include the boundary of numerical integration displayed as a dotted line. The dashed contours are negative contour values, while the solid contours are positive; the zero contour is the first solid contour. Table I presents the oxygen difference electron populations (ΔISEP) determined in the manner described above. Table II lists the analogous Mulliken population differences.

We evaluated the probable error associated with the choice of boundary used by moving the variable-region boundary of integration and then reintegrating for the number of electrons. When this was done for several of the molecules studied, we found a change of 0.001–0.003 e when the boundary was moved 0.2 au left or right of its position as defined by the zero contour. The small magnitude of this number adds validity to our use of difference density maps and changes in oxygen populations and demonstrates the shallow slope of the projection function in the boundary region. This is, in general, not true for atoms closer to the substituent that is being varied. For example, the region around the carbonyl carbon is more complex and includes the bond to a changing substituent; our approach cannot be used to determine ΔISEP values for the carbonyl carbon without serious ambiguities.

A comparison of the integrated oxygen population differences in Table I for the two types of boundaries shows virtually no differences for π electrons. The two values generally differ by no more than 0.001 e. The σ-electron differences show greater variations; the σ variable region was the hardest of the three (π, σ, valence) to define, in the sense that the zero contour "wanders" much more than in either the π or valence cases. Nevertheless, the average difference between variable and fixed boundaries is only 0.005 e, and the maximum is 0.02 e compared to a total effect of substituent ranging from −0.20 to +0.04 e. Clearly, interpretations of substituent effects will not be sensitive to the specific boundaries chosen. Moreover, the valence population changes differ on the average by less than 0.003 e.

In the comparisons to be discussed below, we will concentrate primarily on results from the use of the variable boundaries, since they most clearly reflect the nature of the molecules studied. Nevertheless, because of the close agreement found between fixed and variable population changes, none of the derived conclusions is sensitive to this choice.

Basis Set Dependence

Before reviewing the effects of substituents, it is important to evaluate the 4-31G basis set level used in the present study. Comparison of calculated electron densities with "experimental" values derived from X-ray studies have become increasingly common.[18] Such comparisons are not free from several kinds of difficulties but can be useful tests. For example, the 4-31G basis set reproduces the important features of the "experimental" deformation density of cyanuric acid even though an isolated-molecule calculation is being compared to experimental parameters obtained for a crystal.[19] Both urea and tetracyanoethylene show deformation density peak height discrepancies when compared with 4-31G calculated peak heights; however, it is not known how much of the difference is due to intermolecular interactions present in the experimental work but absent in the calculations.[20] Schweig and Hase[21] have calculated deformation densities for cyanogen by using various basis sets and showed that the 4-31G basis set produces peak heights, when compared to a near-Hartree–Fock basis, that are almost within the "experimental" deformation density error bounds.[22] On the other hand, the STO-3G basis was clearly shown to be inadequate in this study.[21]

To study basis set effects on our oxygen difference populations, we have examined the difference function $P(CH_3CHO) - P(HCHO)$ at the STO-3G, 4-31G, and 6-31G* levels of calculation.[23] Table III lists the variable-region oxygen populations obtained from these maps. The oxygen ΔISEP values do vary somewhat as the basis set is changed. If we assume that the 6-31G* basis produces the best results, then the STO-3G charges are underestimated, while the 4-31G charges are overestimated but are closer to the 6-31G* results. These trends are reasonable; the minimal basis must use the same functions to describe both oxygen lone-pair behavior and C=O bonding density, while the split-valence basis provides some additional flexibility and, indeed, seems

Table III. Effect of Basis Set on Oxygen ΔISEP (P(Acetaldehyde) − P(Formaldehyde))

	STO-3G	4-31G	6-31G*
valence	0.028	0.047	0.038
σ	−0.005	−0.016	−0.011
π	0.033	0.040	0.043

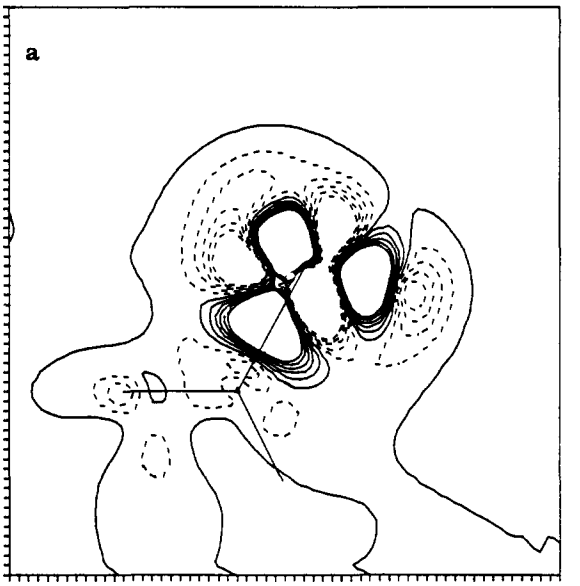

Figure 4. (a) $[P(CH_3CHO) - P(HCHO)]_{6\text{-}31G^*} - [P(CH_3CHO) - P(HCHO)]_{4\text{-}31G}$ for valence electrons. Contours are from −0.005 to 0.005 by 0.001 e/au^2.

(16) A given grid datum actually represents an average value of the projection function at 3600 points over the 0.04-au^2 area of one grid cell and is *not* simply an evaluation of the projection function at that point.[8c] A summation of all of the grid data (for a given grid) yields the total number of electrons in the plot to within 0.00005 e so long as there is no leakage off the edges of the plot.

(17) A complete set of σ, π, and valence projection function difference contour maps, as well as Figure 4, b and c, are available as supplementary material. Ordering information is given on any current masthead page.

(18) Some recent reviews on the subject are as follows: (a) Coppens, P. "Chemical Crystallography"; Robertson, J. M., Ed.; Butterworths: Washington, D. C., and London, 1975; p 21. (b) Coppens, P.; Stevens, E. D. *Adv. Quantum Chem.* **1977**, *10*, 1. (c) Coppens, P. *Angew. Chem., Int. Ed. Engl.* **1977**, *16*, 32.

(19) Scheringer, C.; Kutoglu, A.; Hellner, E.; Hase, H.-L.; Schulte, K.-W.; Schweig, A. *Acta Crystallogr., Sec. B* **1978**, *B34*, 2162–2165.

(20) (a) Scheringer, C.; Mullen, D.; Hellner, E.; Hase, H.-L.; Schulte, K.-W.; Schweig, A. *Acta Crystallogr., Sect. B* **1978**, *B34*, 2241–2243. (b) Hase, H.-L.; Schulte, K.-W.; Schweig. A *Angew. Chem., Int. Ed. Engl.* **1977**, *16*, 257–258.

(21) Hase, H.-L.; Schweig, A. *Angew. Chem., Int. Ed. Engl.* **1977**, *16*, 258–259.

(22) Kutoglu, A.; Scheringer, C. *Acta Crystallogr., Sect. A* **1979**, *A35*, 458–462.

(23) "6-31G*" is a 6-31G basis set with 6 d orbitals on carbon and oxygen; d exponent 0.8 for both carbon and oxygen.

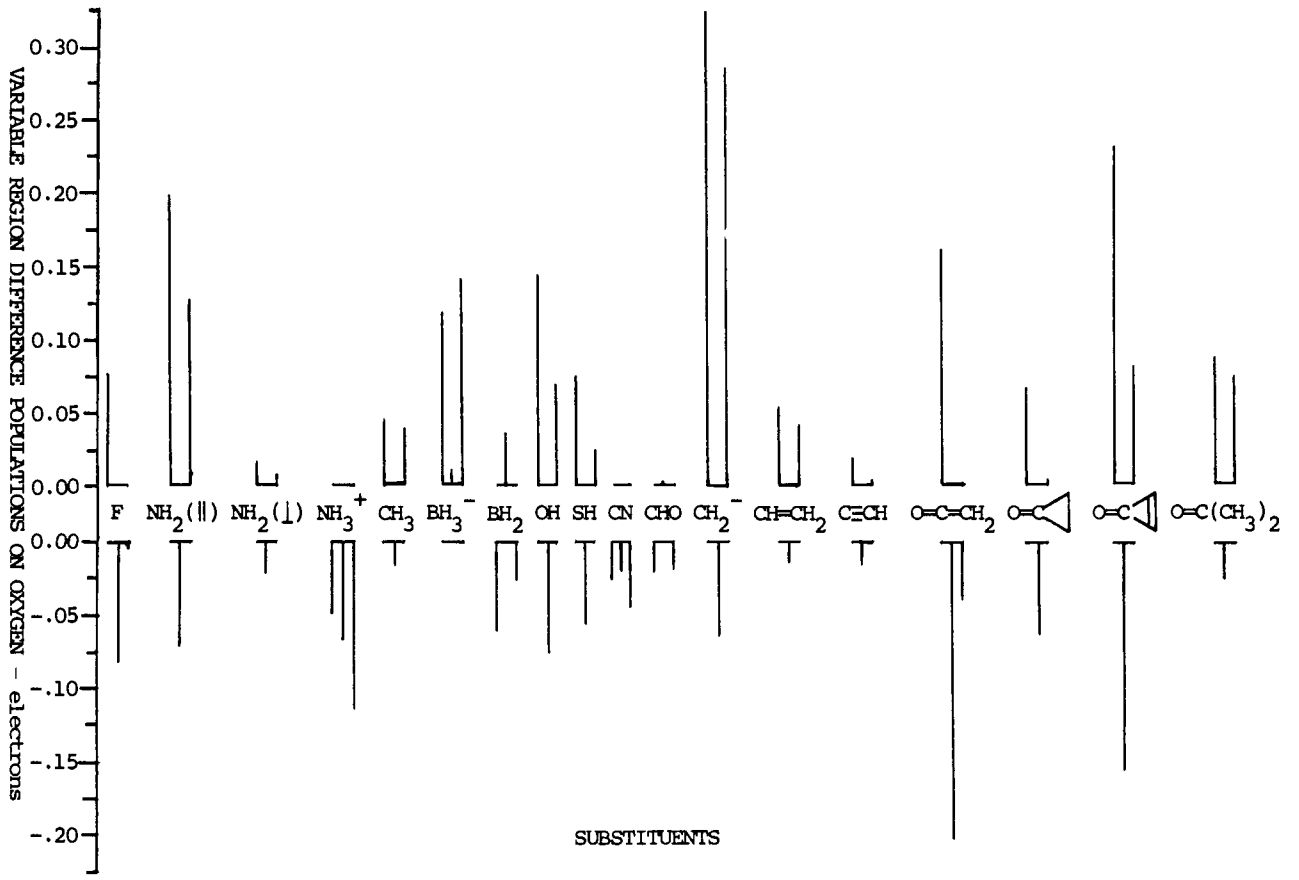

Figure 5. Oxygen ΔISEP bar graph for all molecules studied. For each substituent or molecule shown there are three lines: the left line shows π population, the middle σ, and the right line valence.

to overshoot the mark somewhat. Addition of polarization functions creates a better balanced set of functions, and we see an intermediate result.

In order to visualize the effect of polarization functions, we have plotted in Figure 4a the double difference $[P(CH_3CHO) - P(HCHO)]_{6\text{-}31G^*} - [P(CH_3CHO) - P(HCHO)]_{4\text{-}31G}$ for the valence electrons (Figures 4b and 4c, π- and σ system plots, are available as supplementary material). The negative contours centered on oxygen are a result primarily of π polarization. Below the double bond (opposite the CH_3 group) there is a polarization of electrons away from oxygen and toward the aldehyde C–H bond, which arises primarily from the σ system. Overall, the effects at oxygen itself are rather small, as witnessed by the small contour spacing used to express them: 0.001 e/au^2 (recall that the tick marks on the contour map box represent a spacing of 0.2 au; thus at the 0.001-e/au^2 contour level, a grid square (0.04 au^2) contains only 0.0004 e).

As one would expect, the effect of basis set variation on the *difference* population is small, about the same magnitude as the fixed-region – variable-region difference. Clearly, the 4-31G basis set is adequate for the present comparisons.

Substituent Effects

Figure 5 presents the variable-region ΔISEPs from Table I in graphical form. Most of the results are readily understandable. For example, OH is a strong π donor and σ attractor whereas BH_2 is a strong π acceptor and σ donor. That fluorine is also a strong π donor and σ attractor is expected; what is surprising, however, is that the magnitudes of the two effects are so similar that the net change at the carbonyl oxygen is negligible. We note a recurrent pattern: the σ change is opposite that of the π system and often of lesser magnitude. This effect is interpreted as a dominant effect of the more polarizable π system and a back-reaction or reverse polarization of the σ electrons.[24]

Table IV. σ Parameters

substituent	σ_I	σ_R°
H	0.00	0.00
F	0.49	−0.34
$NH_{2\parallel}$	0.12	−0.48
CH_3	0.02	0.10
$CHCH_2$	0.08	−0.05
CCH	0.30	0.07
CHO	0.25	0.24
NH_3^+	0.60	0.18
OH	0.31	−0.40
SH	0.26	−0.19
CN	0.57	0.08

A comparison of the parallel and perpendicular NH_2 groups is especially instructive. The σ-electron-withdrawing effect of the parallel or conjugating NH_2 is far stronger than that of the perpendicular group and clearly demonstrates the back-polarization effect; that is, the parallel NH_2 nitrogen, having donated π-electron density to the carbonyl oxygen, is effectively more electronegative than the nonconjugating NH_2. This behavior is also seen for the π-accepting substituents; both CN and CHO should also be strong σ acceptors (see Table IV for σ_I parameters); yet because of the σ back-polarization in response to the π system, they withdraw from oxygen only a small number of electrons. In fact, for CHO the σ donation (back-reaction) and normal σ-acceptor ability effectively cancel. The pattern found for $NH_{2\perp}$ probably includes a π-polarization effect similar to that of methyl.

It is interesting to note that the effects of the methyl and vinyl substituents are essentially the same, even though the methyl group acts only to polarize the π system[25] while the vinyl substituent operates by π conjugation. What is more surprising is that the σ effects of the methyl, vinyl, and acetylenyl substituents are all the same, even though hybridization and π-polarization arguments

(24) This effect has been noted before. Pross, A.; Random, L.; Taft, R. W. *J. Org. Chem.* **1980**, *45*, 818–826.

(25) Libit, L.; Hoffmann, R. *J. Am. Chem. Soc.* **1974**, *96*, 1370–1383.

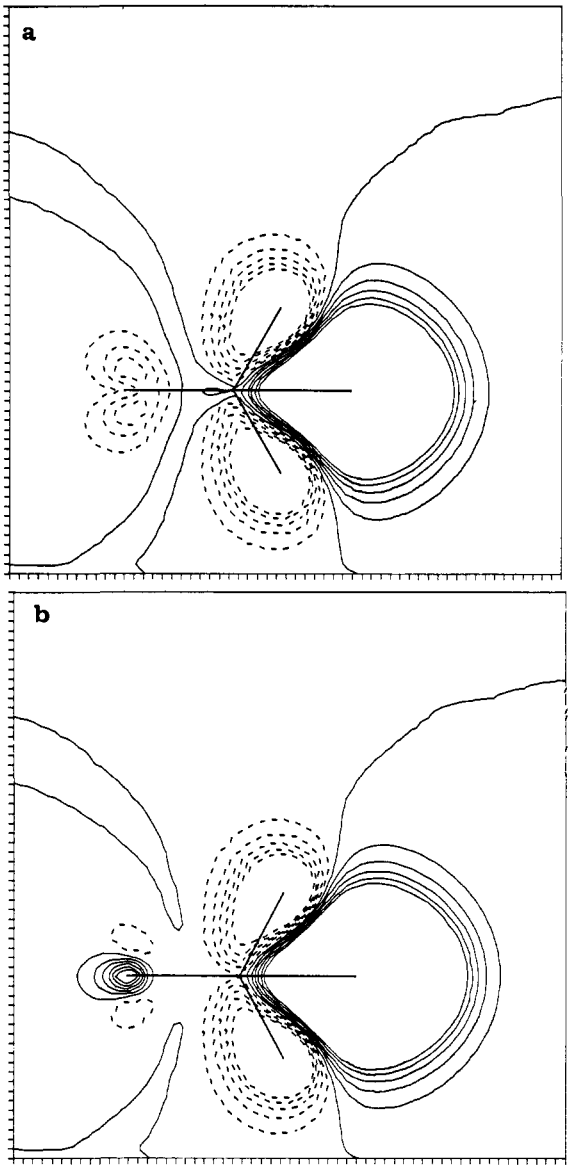

Figure 6. $P(O{=}C{=}CH_2) - P(HCHO)$ for σ electrons. Contours are from −0.10 to 0.10 by 0.02 e/au^2. (b) $P(O{=}C{=}CH_2) - P(HCHO)$ for valence electrons. Contours are from −0.10 to 0.10 by 0.02 e/au^2. The straight lines represent the superposition of ketene and formaldehyde structures with co-spatial carbonyl groups.

would indicate a progression, acetylene being the most electron withdrawing. This is perhaps best rationalized by assuming that the σ effect of the acetylene is "normal" for an sp-hybridized carbon, while those for CH_3 and $CH{=}CH_2$ are augmented by the back-reaction to their larger π effects.

The amount of π donation in the case of propynal is rather small, and even this amount incorporates effects of polarization in the triple bond. The acetylenyl π bond in the carbonyl plane is found by examination of the wave function to polarize away from the carbonyl group, probably in response to the electron deficiency at the β-carbon resulting from normal π donation to the carbonyl oxygen.

Ketene shows the expected effects of a double bond orthogonal to the carbonyl π system but conjugated to an oxygen lone pair. The σ difference map (Figure 6a) shows the bifurcated electron loss at oxygen indicative of major involvement of the in-plane oxygen p orbital. This conjugation produces an effectively more electronegative oxygen and a consequent large back-polarization in the carbonyl π system, much more so than for a normal carbonyl. The combined effect is net loss of electron population at oxygen, but it is important to emphasize that the net change by itself at oxygen leaves unrevealed the pronounced charge transfer from the in-plane oxygen p orbital to the π p orbital, as shown

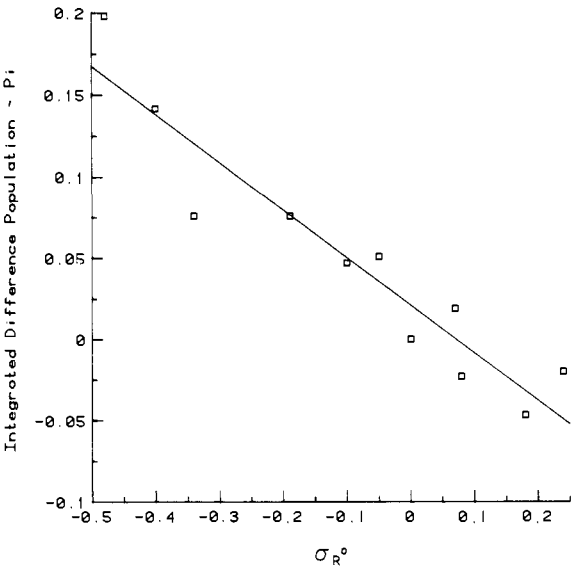

Figure 7. Graph of π ΔISEP vs. σ_R^0. Least-squares slope = −0.293 (± 0.034); intercept = 0.021 (± 0.008); R^2 = 0.893.

clearly in the valence difference plot of Figure 6b. The effect can also be described by the conventional resonance structures Ia–c.

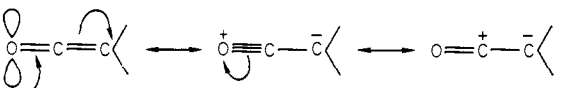

Ia Ib Ic

The effect of two methyl groups is approximately equal to twice that of one CH_3. Tying the two methyl groups together gives cyclopropanone, which has approximately the same π effect but is a much more pronounced σ acceptor. One anticipates that, as part of a three-membered ring, the carbonyl carbon has enhanced s character in its σ bond to oxygen and is thus effectively more electronegative toward the oxygen.

The reason for the "extra" reactivity of cyclopropenone is amply illustrated by Figure 5; except for CH_2^-, it is the strongest π donor of the group. This is, of course, a consequence of the aromaticity to be gained by formation of a partial cyclopropenium cation; that is, Figure 5 is a graphic illustration of cyclopropenium oxide character, IIb. The pronounced σ withdrawal is then largely a consequence of the back-polarization caused by the carbocation character of the ring.

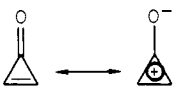

IIa IIb

The trends seen in Figure 5 invite comparison with Hammett-type σ parameters, particularly since Hammett parameters are derived from experiment. We exhibit here the comparison with σ_R^0, a measure of the resonance effect of a substituent, and σ_I, a measure of the inductive strength. Looking only at the 11 substituted aldehydes for which σ_R^0 and σ_I parameters could be obtained[26] (listed in Table IV), we have prepared the graphs shown in Figures 7–9: oxygen ΔISEP = P(YCHO) − P(HCHO) vs. σ_R^0 or σ_I (for the variable regions only).

When π populations are plotted against σ_R^0 (Figure 7), we obtain a reasonable fit (R^2 = 0.89). As expected, there is essentially no correlation between π populations and σ_I: R^2 = 0.11 (this graph is not shown). More surprisingly perhaps, we find no correlation (figure 8) between the σ populations and σ_I (R^2 = 0.12). This lack of correlation undoubtedly is simply one more demonstration that σ_I is primarily a measure of the field effect—a Coulombic effect of a substituent dipole—rather than a measure of intramolecular charge transfer. When σ_R^0 was tried instead

(26) Chapman, N. B.; Shorter, J., Eds. "Correlation Analysis in Chemistry (Recent Advances)"; Plenum Press: New York, 1978; pp 500ff.

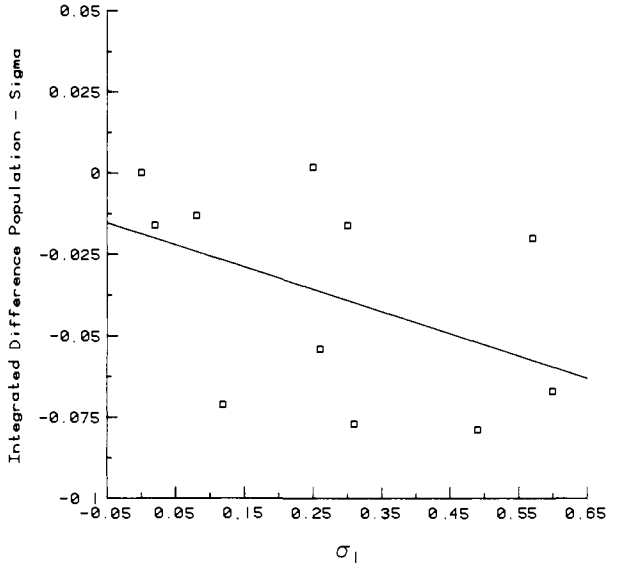

Figure 8. Graph of σ ΔISEP vs. σ_I. Least-squares slope = −0.068 (± 0.046); intercept = −0.019 (± 0.015); R^2 = 0.120.

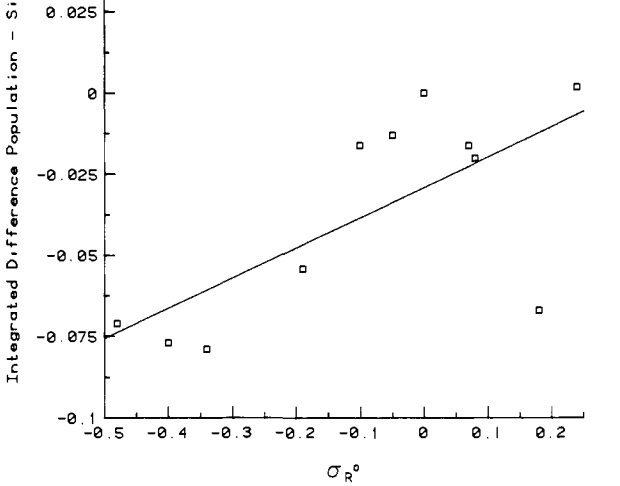

Figure 9. Graph of σ ΔISEP vs. σ_R^0. Least-squares slope = 0.093 (± 0.037); intercept = −0.029 (± 0.008); R^2 = 0.478.

(Figure 9), we obtained a much better fit (although the overall quality is very poor due to a large amount of scatter: R^2 = 0.48). This result supports the earlier interpretation that the σ systems of these carbonyls show mostly a secondary response to the primary effects occurring in the more polarizable π electronic system. In accord with this, the slopes of the two graphs (Figures 7 and 9) are in opposite directions, with the less polarizable σ system having the slope of smaller absolute magnitude.

Comparison with Oxygen 1s (Core) Orbital Energies

It has been shown that the 1s (core) orbital energy of an atom in a molecule is related to the electrostatic potential at that atom.[27] This potential can be related to the charges on all of the atoms in the molecule,[28] the major term being the charge on the atom whose core orbital energy is being investigated. Politzer has found a good correlation between O and F calculated core orbital energies and charges (determined by his technique) for O and F when only neutral diatomic molecules are considered.[7b] For charged molecules, a more complicated equation involving the charges on the other atoms is required in order to approximate the calculated core energies.[7f]

(27) Schwartz, M. E. *Chem. Phys. Lett.* **1970**, *6*, 631–636.
(28) (a) Schwartz, M. E. *J. Am. Chem. Soc.* **1972**, *94*, 6899–6901.

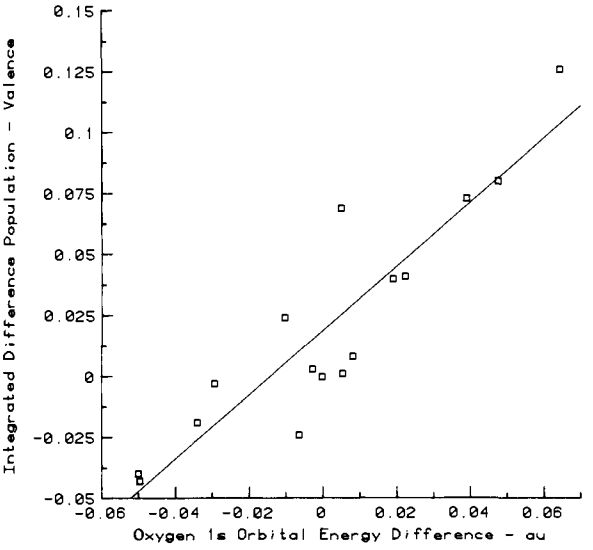

Figure 10. Graph of valence ΔISEP vs. oxygen 1s orbital (core) energy (in au). Least-squares slope = 1.31 (± 0.16); intercept = 0.019 (± 0.005); R^2 = 0.822.

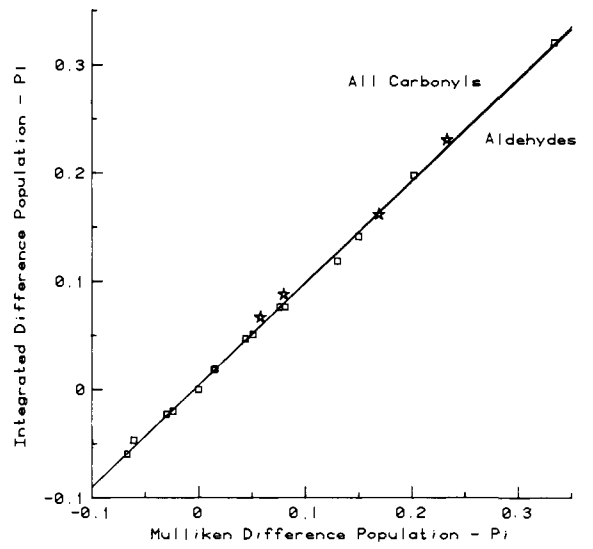

Figure 11. Graph of ΔISEP vs. Mulliken oxygen difference population for π electrons. Aldehydes are denoted by squares, ketones by stars. For all carbonyls: least-squares slope = 0.945 (±0.10); intercept = 0.005 (±0.001); R^2 = 0.998. For aldehydes only: slope = 0.940 (±0.009); intercept = 0.004 (±0.001); R^2 = 0.999.

While we cannot unambiguously calculate charge changes on any other atom but oxygen, it is of interest to determine the degree to which our oxygen difference charges correlate with our calculated oxygen 1s orbital difference energies. Ideally, we would prefer to compare the charge changes with experimental ESCA core energies but few numbers are available for these compounds. The comparison with calculated core energies seems to be a reasonable alternative. Figure 10 shows such a comparison for the variable-region valence changes of our uncharged aldehydes and ketones. As expected, there is a rough correlation (R^2 = 0.82). Unfortunately, the amount of scatter makes it difficult to use this graph as a predictor for the amount of charge on oxygen. To improve the correlation, it would be necessary to include terms for the carbonyl carbon and perhaps for the substituent as well.

Comparison with Mulliken Population Analysis

Finally, we must compare our difference charges with the widely used Mulliken population analysis. Our charges, unlike Mulliken populations, are spatially meaningful and should provide a calibration of the Mulliken technique.

In Figures 11–13 we have graphed our variable-region oxygen difference populations vs. the Mulliken population analysis oxygen

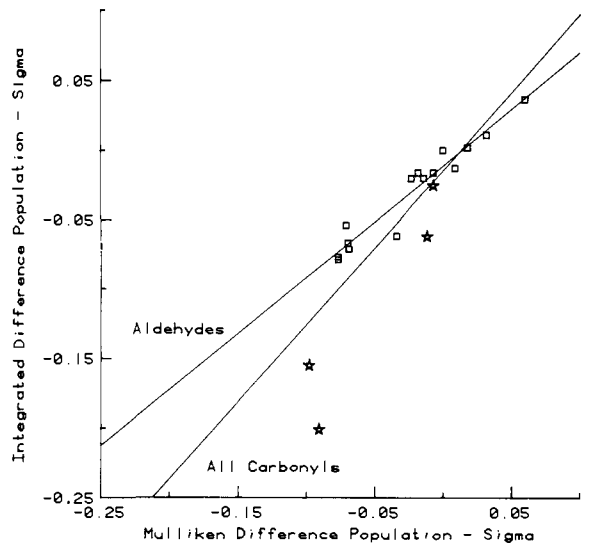

Figure 12. Graph of ΔISEP vs. Mulliken oxygen difference population for σ electrons. Aldehydes are denoted by squares, ketones by stars. For all carbonyls: least-squares slope = 1.11 (±0.16); intercept = −0.015 (±0.008); R^2 = 0.747. For aldehydes only: slope = 0.804 (±0.060); intercept = −0.011 (±0.003); R^2 = 0.932.

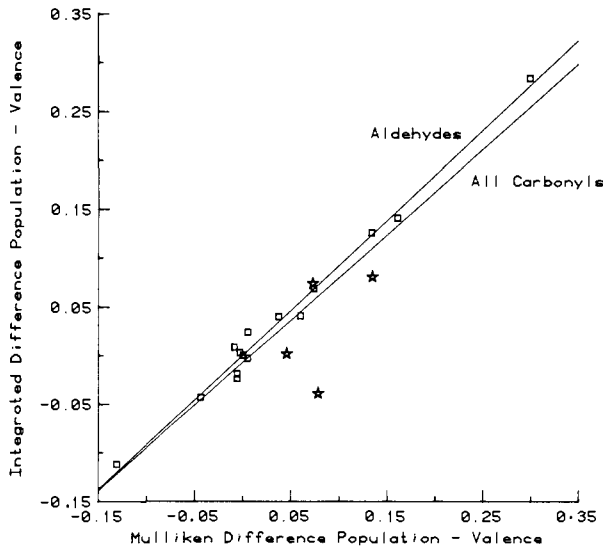

Figure 13. Graph of ΔISEP vs. Mulliken oxygen difference population for valence electrons. Aldehydes are denoted by squares, ketones by stars. For all carbonyls: least-squares slope = 0.873 (±0.078); intercept = −0.008 (±0.008); R^2 = 0.880. For aldehydes only: slope = 0.920 (±0.030); intercept = 0.000 (±0.003); R^2 = 0.986.

difference populations for the π, σ, and valence electron distributions. The figures include separate comparisons for all of the molecules studied (set I) as well as of the substituted aldehydes only (set II). The corresponding graphs for the fixed region were also determined but are not reproduced here. They are practically identical with the variable-region graphs and have, within one standard deviation, the same slopes and intercepts.

The π- electron correlation is excellent for both sets of molecules: R^2 = 0.999. In each case the slope is slightly less than unity; this difference seems significant in light of our slope standard deviations. Unfortunately, since our definition of atomic charge is a *difference* definition, we cannot compare directly a given oxygen Mulliken population with the same projection function population. Thus the exact cause of the nonunity slope is unknown[29] but undoubtedly involves the way in which the "overlap density" is apportioned.

(29) We have observed this nonunity slope when the same type of comparison is made with substituted benzenes.

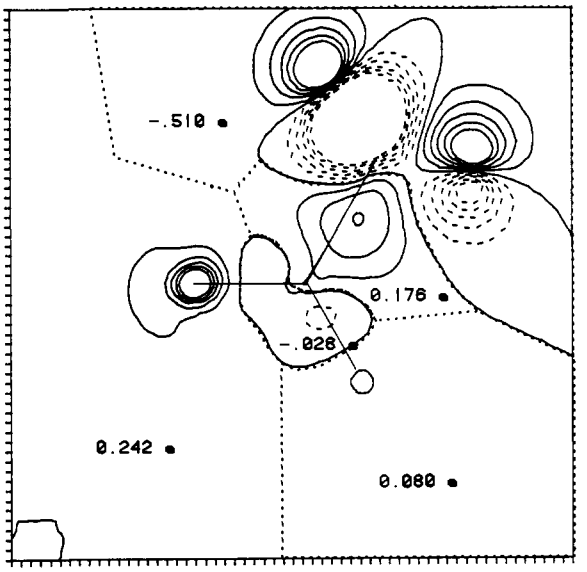

Figure 14. $P(CHOCH_2^-) - P(CHOCH_3)$ for valence electrons. Contours are from −0.10 to 0.10 by 0.02 e/au^2. Numbers printed on the map indicate the number of electrons within the various dotted integration boundaries.

The σ population correlation is much poorer than that of the π case, especially with the set I molecules cyclopropenone and ketene. With set II a reasonable correlation is found (R^2 = 0.93), again with a slope smaller than unity; note that the deviation from unity is larger in this case. While some of the scatter in this line is probably due to an inadequate definition of the region that we have integrated (especially for NH_3^+, $NH_{2\perp}$, and CN), many of the remaining aldehydes have σ regions as well-defined as those in the π system; one would assume that the σ results are just as valid. The large scatter in this fit and the smaller-than-unity slope both point out an inherent inability of the Mulliken population analysis to correctly apportion σ system electron density; that is, basis set populations cannot generally be equated to spatial populations. Overlap integrals in π systems are generally smaller than for σ systems; hence, the effects of the arbitrary Mulliken apportionment are less significant. The above results suggest that Mulliken populations may be expected to be relatively reliable for regions separated by low-density contours if the basis is not seriously overweighted in diffuse functions.

The valence graphs are, as one would expect from a direct summation of π and σ, intermediate between them in goodness of fit; R^2 = 0.986 for set II, with a slope between that of π and σ. The set I correlation is poorer, again because of cyclopropenone and ketene.

Our results indicate that the Mulliken analysis is an excellent indicator of π-electron *difference* populations and provides reliable trends for σ population differences. Of course, in the carbonyls studied here, the σ changes are generally less than those in the π system; in nonconjugated molecules the conclusions above may change or even reverse.

Whole-Molecule Comparison: Enolate Minus Acetaldehyde

The bulk of this paper has dealt only with charges defined around the carbonyl oxygen and not with charges or interpretations of contour map changes in other regions of the molecule. There is a very good reason for this, of course: the (substituent H) region swamps out the subtle effects one would like to observe. However, by fixing the C–C bond length in the enolate anion ($^-CH_2CHO$) to be the same as that in acetaldehyde, we are able to examine the changes that occur when acetaldehyde is deprotonated to form the planar enolate anion. Clearly, fixing the C–C bond length in this way is an artifact, and the absolute electron difference populations obtained in this manner will not be very reliable; however, significant trends should still be apparent.

Figures 14–16 show the valence, σ, and π contour maps (P(enolate) − P(acetaldehyde)). The valence map is perhaps the most interesting and shows approximately what one would expect

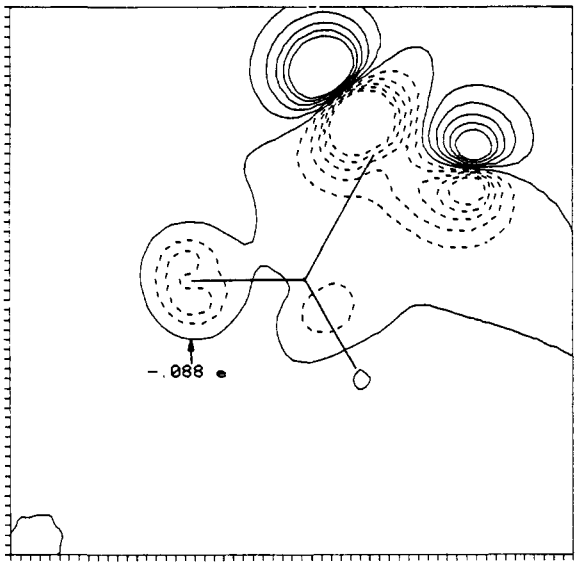

Figure 15. $P(CHOCH_2^-) - P(CHOCH_3)$ for σ electrons. Contours are from −0.10 to 0.10 by 0.02 e/au². The number of electrons about oxygen is printed on the map; the integration boundary is not shown but follows the zero contour about oyxgen.

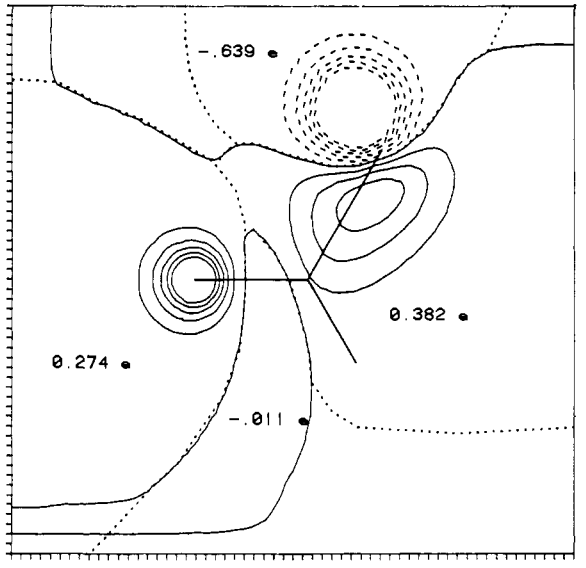

Figure 16. $P(CHOCH_2^-) - P(CHOCH_3)$ for π electrons. Contours are from −0.10 to 0.10 by 0.02 e/au². Numbers printed on the map indicate the number of electrons within the various dotted integration boundaries.

from the simple exercise of drawing resonance structures for the enolate anion: a large buildup of charge density on oxygen and in the C–C bonding region, which occurs at the expense of the CH_2^- group. The changes in the far upper right of Figures 14 and 15 are not important since they represent movement of hydrogens. What is remarkable is that there is only a slight decrease of density in the C=O bonding region, in both the valence and π maps; this result is not apparent in either classical resonance structures or simple Hückel approaches. The aldehydic C–H bond is weakened slightly; density at that hydrogen has actually increased slightly.

Conclusion

We have presented a definition of difference charge density, based on an analysis of projection function difference density contour maps. This is a *difference density* definition, in which the exact position of the spatial boundary is relatively unimportant, because of the shallow contours in the region chosen as the boundary.

We have applied this definition to the oxygen of various substituted aldehydes and ketones and have examined the effects of the various substituents on that oxygen. We find that the π system generally behaves as expected and that the dominant feature in the σ system is a "back-reaction" to the more polarizable π system.

We have found that for the π populations, we obtain essentially the same results as the Mulliken population analysis. For σ and valence electron densities, Mulliken populations show the same general trends but differ significantly for some structural changes. We believe our results to be superior since they are based upon actual regions in space rather than on an arbitrary partitioning of the basis functions used in the calculation. Because of this fact, conclusions about substituent effects are expected to be more reliable than those based solely upon Mulliken populations.

We find a rough correlation of our σ, π, and valence difference charges with σ_R^0, a σ parameter that is supposed to measure only the resonance contribution of a given substituent. We find virtually no correlation with σ_I, a purely inductive parameter; the carbonyl group is strongly dominated by conjugation or π interactions.

It was thought that oxygen 1s orbital energies might be used to predict our difference charges; not unexpectedly, we find that these core energies can be used only to predict trends and do not correlate with our oxygen charges nearly as well as Politzer's diatomic systems.

Finally, we have applied the projection function technique toward the study of an entire molecule: the enolate anion. Such a study is only possible when the two molecules being compared are structurally identical in the region of interest, for example, with their heavy atoms (and preferably hydrogens as well) in the same positions relative to one another. Consequently, we have had to introduce a perturbation into one of the molecules (lengthening the enolate C–C bond). In this type of comparison lies the true strength of the projection function technique: in isoelectronic systems such as these, we know that any loss of charge density in one region of the contour map *must* be compensated by a corresponding gain in density in some other region(s) of the map.

Acknowledgment. This work was supported in part by National Science Foundation Grant CHD79-10814. Additional computer time was provided by the Office of Computing Affairs, University of California.

Registry No. H—CHO, 50-00-0; F—CHO, 1493-02-3; H_2N—CHO, 75-12-7; H_3N—CHO^+, 50785-80-3; H_3C—CHO, 75-07-0; H_3B—CHO^-, 81740-96-7; H_2B—CHO, 32375-83-0; HO—CHO, 64-18-6; HS—CHO, 16890-80-5; NC—CHO, 4471-47-0; OHC—CHO, 107-22-2; H_2C—C^-—HO^-, 64723-93-9; H_2C=CH—CHO, 107-02-8; HC≡C—CHO, 624-67-9; ketene, 463-51-4; cyclopropanone, 5009-27-8; cyclopropenone, 2961-80-0; acetone, 67-64-1.

Supplementary Material Available: A complete set of σ, π, and valence projection function difference contour maps, as well as Figure 4, b and c, are available as supplementary material (22 pages). Ordering information is given on any current masthead page.